Unexpected Stable Stoichiometries of Bismuth Sulfide under High Pressure and High Temperature

Guangtao Liu[1, 2, 3], Zhenhai Yu[1], Hanyu Liu[4], Yanmei Ma[3], Hui Wang[3], Xiaolei Feng[3], Yanming Ma[3], Xin Li[1], Ye Yuan[1], Lin Wang[1], Ke Yang[5] and Xiaodong Li[6]

[1] *Center for High Pressure Science and Technology Advanced Research, Shanghai 201203, China*

[2] *National Key Laboratory of Shock Wave and Detonation Physics, Institute of Fluid Physics, China Academy of Engineering Physics, Mianyang 621900, China*

[3] *State Key Laboratory of Superhard Materials, Jilin University, Changchun 130012, China*

[4] *Geophysical Laboratory, Carnegie Institution of Washington, Washington, DC 20015, USA*

[5] *Shanghai Institute of Applied Physics, Chinese Academy of Sciences, Shanghai 201203, China*

[6] *Institute of High Energy Physics, Chinese Academy of Sciences, Beijing 100049, China*

Abstract

Normally, bismuth-sulfur binary system always crystallizes in stoichiometric Bi_2S_3 with excellent functional properties. In this paper, combining the crystal structure prediction method and first principles calculations, we extensively explored the structural stabilities of other Bi-S compounds under high pressure. We theoretically predicted that unconventional semi-metallic layered BiS_2 and metallic body-centered cubic BiS can be synthesized above 9 and 19 GPa, respectively. Furthermore, with laser heating and in-situ x-ray diffraction, we successfully confirmed that Bi_2S_3 decomposed into Bi and BiS_2 in the diamond anvil cell experiments. Our additional electron-phonon coupling calculations indicate that the superconductivity exists in Bi-S compound. These studies shed light on a way for the design and synthesis of new functional V-VI group compounds with counterintuitive stoichiometries and new structures at extreme conditions.

I. Introduction

The binary V-VI group compounds, such as Bi_2Se_3, Bi_2Te_3, and Sb_2Te_3, have attracted significant research interest in recent years, in particular focusing on their three-dimensional topological behavior, excellent thermoelectric properties and superconductivity. First, Bi_2Se_3, Bi_2Te_3, and Sb_2Te_3 were predicted to be 3-dementional topological insulators, which have robust and simple surface states consisting of a single Dirac cone at the Γ point [1]; the surface state of Bi_2Te_3 was subsequently confirmed by angle-resolved photoemission spectroscopy experiment [2]. Furthermore, compression plays an important role in tuning these materials and their physical properties, which are mainly governed by their crystal structures. For example, it has been found that the thermoelectric properties of Bi_2T_3 and Sb_2Te_3 improve remarkably [3,4] at high pressures. The superconducting temperature (T_c) of ~3 K was observed between 3 to 6 GPa in Bi_2Te_3, indicating the possibility that the bulk state could be topological superconductor. [5] Further experimental studies indicated that superconductivity in Bi_2Te_3 shows variation at high pressures, which may be correlated to its high-pressure phase transitions. [6] Subsequently, it has been reported that Bi_2Te_3 undergoes a series of structural phase transitions from an ambient pressure *R*-3*m* phase to a *C*2/*m* phase, then to a *C*2/*c* structure, accompanied by an increase in coordination number from 6 to 7/8, and finally 9/10 [7,8]. The same (or similar) high-pressure phase transitions have been observed in Sb_2Te_3 [9,10] and Bi_2Se_3 [11–13].

In addition to inducing phase transitions, high pressure can also modify chemical behavior and lead to the stabilization of new compounds with novel properties. It enables us to uncover new physical and chemical processes that illuminate our understanding of the nature of the materials more generally. Thus far, many computational and experimental studies have reported the occurrence of unexpected compounds with new structures that are stabilized at high pressures, but which cannot occur at ambient pressure. For instance, intriguing Cs-F [14], and Hg-F [15] compounds were predicted to be stable under compression on the basis of computational results. Subsequently, some of these predictions (Xe_3O_2 [16,17], $XeNi_3$ [18,19], NbH_3 [20,21], $NaCl_3$/Na_3Cl [22], Sn_3Se_4 [23] etc.) have since been confirmed by successfully synthesized materials observed experimentally at extreme conditions. Other than the well-known A_2B_3-type structures, which are important both in fundamental science research and in practical applications, so far no group V-VI compound has been reported. Here, we investigate the possibility that other, as yet unknown, stable compounds exists in this significant group. Such structure prediction could, for example, yield materials with improved materials properties, which could potentially be synthesized and developed for potential future application. Initially, the well-known Bi-S system has been chosen for study as representative of group V-VI compounds more generally.

At ambient pressure, Bi_2S_3, bismuthinite, is a typical semiconductor with direct bandgap of ~1.3-1.9 eV [24,25] and finding applications in thermoelectric [26], electronic [27] and optoelectronic devices [28]. Bismuthinite crystallizes in an orthorhombic structure with space group *Pnma* (Z=4) [29], [30] in which Bi is irregularly coordinated by S in two distinct crystallographic sites, with 7- and 8-fold irregular coordination. High-pressure x-ray diffraction (XRD) investigations found that bismuthinite retains *Pnma* symmetry up to 50 GPa above which point a disordered or amorphous phase was proposed to exist. A possible second-order isosymmetric transition in the *Pnma* phase was suggested to occur around 4-6 GPa [31]. Furthermore, a pressure-induced semiconductor-metal transition in Bi_2S_3 was indicated at around 20 GPa from measurements of the temperature dependence of its electrical resistance. [32]

Here, we report the results of our systematic theoretical and experimental studies on Bi-S system in an exploration of a the new compound found in the binary system at high pressures. We explore variable chemical compositions of Bi_xS_y using the crystal structure prediction methods combined with first principles calculations. Enthalpy calculations indicate that Bi_2S_3 tends to spontaneously decompose above 24 GPa into two new phases with stoichiometries BiS_2 and BiS, which have abnormal valence states and should become enthalpically stable above 9 and 19 GPa, respectively. Using diamond anvil cell (DAC) and laser heating techniques, we have successfully observed our predicted BiS_2 phase during high-pressure/high-temperature experiments. We also suggest that metallic BiS displays a superconducting transition at low temperature and BiS_2 shows a semi-metallic behavior, on the basis of our density functional theory (DFT) calculations.

II. Computational and experimental details

The crystal structures of Bi-S compounds were systematically probed using the Crystal structure AnaLYsis by Particle Swarm Optimization (CALYPSO) code [33,34], which is based on a global minimum of search of free energy surfaces calculated by the DFT total energy calculations. The simulation cell comprised of one to eight formula units (equivalent to 24 atoms) with six stoichiometries (Bi_2S, BiS, Bi_2S_3, BiS_2, Bi_2S_5, and BiS_3) at 10, 40, and 60 GPa. Generally, the search was terminated after the generation of 2000-2500 structures. DFT calculations, including structural optimizations, enthalpies, electronic structures and phonons, were performed with Vienna Ab initio Simulation Package (VASP) [35] code using the Perdew-Burke-Ernzerhof [36] exchange-correlation functional. The $6s^26p^3$ and $3s^23p^4$ electrons were treated as valence electrons for Bi and S, respectively. To ensure that all enthalpy calculations were well-converged to about 1 meV/atom, a Monkhorst-Pack grid was selected with sufficient density ($2\pi\times0.02$ $Å^{-1}$) in reciprocal space, as well as appropriate energy cutoff (350 eV). The phonon

calculations and modulations of soft phonon modes were carried out using a finite displacement approach [37] through the PHONOPY code [38], which uses the Hellmann-Feynman forces calculated from the optimized supercell through VASP. Molecular dynamics (MD) calculations based on VASP were performed with a constant volume and temperature (NVT) ensemble at 300 K, where the supercell containing 192 atoms was calculated over a total time of 10 ps with the step of 1 fs. Electron-phonon coupling (EPC) calculations were performed using density functional perturbation theory. Norm-conserving pseudopotentials for Bi and S were adopted with a kinetic energy cutoff of 100 Ry. A K-mesh of 16×16×16 and q-mesh of 8×8×8 and for the the first Brillouin zone (BZ) of the BiS structure was used in the EPC calculations with the Quantum Espresso package [39].

High-pressure/high-temperature synthesis experiments were carried out using the laser-heared diamond anvil cell (DAC), with direct observation using synchrotron X-rays. Pressure was generated using a DAC with culet diameter of 300 μm. A gasket of T301 steel, thickness 250 μm, was pre-indendented and provided the sample chamber. Bi_2S_3 powder from Alfa Aesar (99.9% purity) was prepressed into a thin sheet (~ 10 μm) and then loaded between two layers of MgO to form a sandwich structure, where MgO was used as both the thermal insulator and pressure medium. Pressures were determined by the ruby fluorescence method [40]. An ytterbium fiber laser (1064 nm excitation line) was used to heat the sample. Temperatures were measured by fitting the visible portion of the black-body radiation from the heating spot on the sample to the Planck radiation function. Room-temperature X-ray diffraction (XRD) measurements were performed principally at beamline 15U1 of the Shanghai Synchrotron Radiation Facility using monochromatic X-rays of wavelength λ = 0.6199 Å. Some additional experiments were condicted at the 4W2 High Pressure Station of the Beijing Synchrotron Radiation Facility. A 2D image plate detector recorded powder diffraction patterns. The sample to detector distance and other geometric parameters were calibrated using a CeO_2 standard. The software package Dioptas [41] was used to integrate powder rings and convert the 2-dimensional data to 1-dimensional diffraction profiles.

III. Results and discussions

To validate our computational prediction method and DFT calculations on the Bi-S system, we successfully reproduced the known orthorhombic (*Pnma*) bismuthinite structure of Bi_2S_3 at both atmospheric pressure and 10 GPa using the Particle Swarm Optimization (PSO) search. We were also able to reproduce the known equation of state, verifying the reliability of our methodology. We then extended our approach to consider more stoichiometries that were explored as a function of pressure. The formation enthalpy of each phase at each stoichiometry can be defined as

$$H_{f/atom} = \frac{H_{Bi_xS_y} - x\,H_{Bi/atom} - y\,H_{s/atom}}{x+y}$$

where the *R*-3*m* and *Im*-3*m* phases [42] were used for Bi, and the *α*, *P*3$_2$21 and *I*4$_1$/*acd* phases [43] were employed for S as the endpoint compositions, at the appropriate pressures. Here, the zero-point energy is not considered since it is expected to be an insiginificant and negligible contribution in view of the heavy element nature of these materials. The enthalpic convex hulls, showing enthalpoes as a function of pressure, were calculated and are summarized in figure 1, where the points on the convex extrema are stable stoichiometries. At ambient pressure, it we find (reasonably) that the only stable phase is the one with Bi:S ratio of 2:3, confirming the reliability of our method yet again. At elevated pressures, BiS_2 and BiS become energetically stable at 9 and 19 GPa, respectively. Furthermore, their energies become lower than that of the known bimsuthinite phase, Bi_2S_3. Above 24 GPa it is apparent that Bi_2S_3 tends to decompose above 24 GPa (figure 1-insert), according to the reactions:

$$\text{(i) } Bi_2S_3 \rightarrow 2BiS + S, \text{(ii) } Bi_2S_3 \rightarrow \tfrac{3}{2}BiS_2 + \tfrac{1}{2}Bi \text{ , (iii) } Bi_2S_3 \rightarrow BiS + BiS_2.$$

The decomposition pathway depends on the, as yet unmeasured, potential energy surface of this system, which is beyond the scope of our present study.

In addition to the calculations of the enthalpies of these structures, we have also calculated the phonon dispersion curves of BiS and BiS_2 (Figure 2). For the simple cubic (sc) BiS structure, no imaginary phonon frequencies were found across the Brillouin zone (BZ), confirming the dynamic stability of this structure (Figure 2a). However, phonon calculations of the newly-predicted BiS_2 structure (*Cmca*, 8 f.u./cell) reveal a soft phonon branch with negative frequencies running from the U-point (0, 0.5, 0.5) to the R-point (-0.5, 0.5 0.5) of the BZ (Figure 2b), indicating that this structure is dynamically unstable and that an alternative structure should exist. It is difficult to identify this crystal structure by simply searching across the complicated potential energy surface, so instead we have identified it by modulating the structure of the *Cmca* BiS_2 phase. We did so by adding displacements corresponding to the wavevector of the U-point within a supercell of *Cmca* structure, to obtain a structure with space group of *P*2/*m* (16 f.u./cell). We find that the structural topologies of the *Cmca* and *P*2/*m* phases are very similar. Compared to the *Cmca* structure, the layers of atoms (Bi or S) are distorted in the *P*2/*m* structure. In addition, phonon calculations reveal that the *P*2/*m* structure is dynamically stable (Figure 2c), with an energy is ~ 3 meV/f.u. lower than that of the *Cmca* structure. Furthermore, MD simulation also show that this structure experiences no additional structural change after relaxation. Therefore, it is safe to conclude that the modulated *P*2/*m* structure is the ground state of BiS_2.

The stable crystal structures of each stoichiometry within the Bi-S binary at 20 GPa are shown in Figure 3.

The familiar bismuthinite structure of Bi_2S_3 (*Pnma*) is composed of stacked irregular BiS_7 co-ordination polyherda (Figure 3a). The sc structure of BiS (*Pm*-3*m*), on the other hand, comprises stacked with regular BiS_8 hexahedra (Figure 3b). Finally, BiS_2 adopts a monoclinic structure formed by BiS_9 triskaidecahedra, and can be described as a layer-liked structure with a stacking sequence ⋯S-Bi-S-S-Bi-S-Bi-S-S-Bi-S⋯ along the *b*-axis (Figure 3c). Typically, increasing pressure results in crystalline materials becoming denser and trending towards close-packed arrangements, with a concomitant increase in coordination number of atoms or ions. Our results show that, in these Bi-S compounds, the coordination of Bi by S increases from 7 (Bi_2S_3) to 8 (BiS) or 9 (BiS_2) during pressure-induced decomposition. However, this increase in coordination number results in an increase in the average bond length, despite the increase in pressure. For example, at 20 GPa the inter-atomic distances of the Bi-S bond changes from 2.68-2.75 Å in Bi_2S_3 to 2.92 Å in BiS and 2.75-2.96 Å in BiS_2. This can be understood in terms of the enhancive repulsive interactions between nearest neighbor atoms arising from the increase in coordinating S atoms. Interestingly, we observe that covalent S-S bonds (2.04 Å) exist in BiS_2, as depicted in figure 3c, which is exceedingly close to value of 2.08 Å for the S-S covalent bond seen in the in the chain-structure of elemental S-II ($P3_221$) at 20 GPa.

To confirm the theoretical predicted stoichiometries given by our ab initio computational results, further high-pressure experiments were performed to synthesize compounds across the Bi-S composition range, including (in particular) BiS_2 and BiS. The starting material was a well-characterized sample of bismuthinite, Bi_2S_3, that was checked carefully before heating to confirm the absence of any Bi impurity [see Supplemental Material (SM)]. In addition to compression, high temperature is necessary to induce the thermally-activated high-pressure breakdown of bismuthinite. The sample was, therefore, heated to 1800 K at 31 GPa for 30 minutes, following which the pressure was decreased to 24.5 GPa and finally the sample was cooled down. Then the sample was then compressed to 38 GPa and heated up to about 2000 K for another 30 minutes in a second run. The pressure was then decreased to 31.5 GPa after laser heating. The quenched sample was scanned by an x-ray beam in order to investigate any heterogeneity caused by the temperature gradient. XRD mapping results showed that many new grains had formed with a typical length scale of several μm. We note that the experimental intensities of XRD patterns were dominated by obvious texture and pseudo-single crystal statistics (rather than powder) after the experiments that had provoked rather coarse recrystallization from high temperature. Clear diffraction peaks of a body centered cubic (bcc) structure were observed in certain parts of the sample, which were identified as bcc Bi. In addition to bcc Bi, at least two additional phases were always observed. Using the results of the computational structure predictions we were able to test these structures against those predictions, and we were able to conclude

that the Bi_2S_3 may have decomposed into Bi and BiS_2. Fortunately, apart from a number of unidentified peaks, most of the diffraction patterns at 31.5 GPa can be explained accurately by the model of our predicted BiS_2 ($P2/m$) and bcc Bi (Figure 4a). The residual unidentified peaks (indicated by question marks) may be from additional unconsidered metastable phase(s), possibly of stoichiometry beyond our current calculations arising from the complicated chemical interactions within the sample assembly at high pressure and high temperature. We find compressibility of Bi that is highly consistent with the previously-reported equation of state of Bi [44] (Figure 4b), further supporting the existence of decomposed Bi. The reduction in pressure after heating contributes to the obvious volumetric collapse upon decomposition. Newly-formed BiS and BiS_2 are denser and more incompressible than the original bismuthinite, Bi_2S_3, as is indicated by their equation of states and elastic moduli [SM]. Encouraged by the successful observation of BiS_2, we also suggest that sc BiS could be synthesized with S and excessive Bi at moderate temperature and pressure.

Since it is difficult to control chemistry with the DAC to obtain pure phases by laser heating techniques, the electronic properties of BiS and BiS_2 were investigated by first principles calculations. Because DFT usually underestimates the band-gap of materials, we employed the screened hybrid functional of Heyd, Scuseria, and Ernzerhof (HSE06) [45] to better describe the band structure and density of states (DOS) of our predicted BiS and BiS_2 high pressure phases. In BiS (figure 5a), the valence bands and conduction bands completely overlap indicating a metallic state, which is in consistent with the high DOS at the Fermi level. From the projected DOS, we find that most of the electronic states below the Fermi level are associated with the S_3*p* electrons, but also partly by Bi_6*s* and Bi_6*p* orbitals; above the Fermi level, the main contribution is from the Bi_6*p* and S_3*p* orbitals. The valence band of BiS_2 is occupied by S_3*p* (Figure 5b). It can be seen that there is slight overlap along the T-Y direction and that the DOS is near zero at the Fermi level, indicating that BiS_2 is a semi-metallic phase. The diverse electronic properties can be understood intuitively in terms of the different concentrations of nonmetallic S in these phases, which leads to a reduction in electron transfer from Bi to S in metallic BiS. Thus, the delocalized electrons enhance the conductivity in BiS.

Experimental observations indicate that the superconductivity arises in Bi_2Te_3 [5,6], while there have been no repsorts of superconductivity in Bi_2S_3 to date. The Bi-S compounds, none the less, have the potential to show superconductivity as a function of chemical compositions or pressure at extreme conditions. Thus, we performed the EPC calculations on metallic BiS to explore its possible superconductivity. In these calculations, the Gaussian broadening was set to 0.03 Ry and the critical temperature T_c was calculated via the Allen-Dynes modified McMillan equation [46]:

$$T_c = \frac{\omega_{log}}{1.2} exp\,[-\frac{1.04(1+\lambda)}{\lambda - \mu^*(1+0.62\lambda)}]$$

Where λ is the first reciprocal moment of $\alpha^2F(\omega)$,

$$\lambda = 2\int_0^\infty \frac{\alpha^2 F(\omega)}{\omega} d\omega$$

ω_{log} is the logarithmic average frequency and, μ^* is the empirical Coulomb pseudopotential.

$$\omega_{log} = exp[\frac{2}{\lambda}\int \frac{\alpha^2 F(\omega) log\omega}{\omega} d\omega]$$

Using the obtained Eliashberg spectral function $\alpha^2F(\omega)$ and the total EPC parameter λ (Figure 6a), the critical temperature was estimated to lie between 9.3 and 10.6 K at 20 GPa with typical values of μ^* ranging from 0.1 to 0.13. Our λ integration show that ed all vibrational modes contribute to T_c. Moreover, the calculated T_c was found to decrease slowly over its stable range of pressures (Figure 6b). These calculations inform our understanding of the properties of these materials and we anticipate that the electrical properties and superconductivity will be measured in the future, as soon as pure stpichiometric BiS can be synthesized.

Earlier studies have suggested that the significant V-VI group compounds can show complex high-pressure structural evolution. Compared to many V-VI compounds, Bi_2S_3 seems more stable and robust, maintaining structural stability to high pressure. In contrast, Bi_2Te_3 shows alloying order-disorder behavior, withe almost equal atomic radius (r_{Bi}/r_{Te} ~ 0.97 at 20 GPa [7]) and electronegativity between Bi and Te, which meet the Hume Rothery Rules under compression. Our experimental work on the Bi-S system encourages us to believe that, besides the A_2B_3-bimsuthinite structure type, many undiscovered structures with interesting and potentially useful properties may exist among the V-VI group compounds,. High-pressure and high-temperature techniques will be particularly valuable in the search for such structural variability. For instance, by substituting S by Te in the sc BiS (*Pm*-3*m*) phase we can extend our observations to consideration of the stability of the Bi-Te system. Although the other stoichiometries have not been considered here, our energy calculation indicate that, at least, 9/10 fold-coordinated Bi_2Te_3 is thermodynamically unstable within the convex hull [SM] of this system and sc BiTe has a lower energy at 30 GPa (Bi_2Te_3 → 2 BiTe + Te + 0.037 eV). The calculated lattice parameter of sc BiTe is 3.597 Å at 26 GPa, matching the experimentally reported value for cubic Bi_2Te_3 (3.571 Å) very closely. Thus, the observed substitutional alloy can be better understood according to the following perspective: compression induces Bi_2Te_3 to decompose into Te and sc BiTe, where 20 % Bi is replaced by redundant Te ($Bi_{0.8}Bi_{0.2}Te$ → $Bi_{0.8}Te_{0.2}Te$). At the same time, the observed cubic phase in Bi_2Te_3 indirectly supports our prediction that the sc AB-type structure is stable in the Bi-S system. It seems likely, therefore, that previously unreported stoichiometries exist widely within the V-VI group of compounds, which can be engineered or controlled by tuning these compositions under

compression. It should noted that variations of stoichiometry need to be carefully considered in high pressure calculations and studies, especially in cases with additional high temperature.

IV. Conclusions

In summary, we have carried out systematic investigations into compounds that exist across the Bi-S binary system using a PSO algorithm approach under high pressure. Two new stoichiometric BiS and BiS_2 compounds are predicted to be stable above ~9 and 19 GPa, respectively, whereas conventional bismuthinite Bi_2S_3 should decompose only sbove about 24 GPa, as we have verified through synchrotron XRD experiments of samples in the laser-heated DAC. Eight-fold coordinated (Bi by S) sc BiS and layered nine-fold BiS_2 are more densely packed compared to seven-fold coordinated Bi_2S_3. Electronic structure calculations indicate that the new BiS_2 compound shows semi-metallic behavior. Our calculations based the Bardeen–Cooper–Schrieffer theory predict that metallic BiS shows a superconducting transition at ~ 10 K under 20 GPa pressure. Our results demonstrate that as well as the familiar A_2B_3-type V-VI compounds, other unexpected stoichiometries may be stable and that these may show interesting properties, and are generally stabilised under compression. High-pressure studies can provide new insights into the design, exploration, and ultimately synthesis of novel materials with unusual chemistry and potentially useful properties..

Acknowledgments

We are grateful for…

Figures and captions

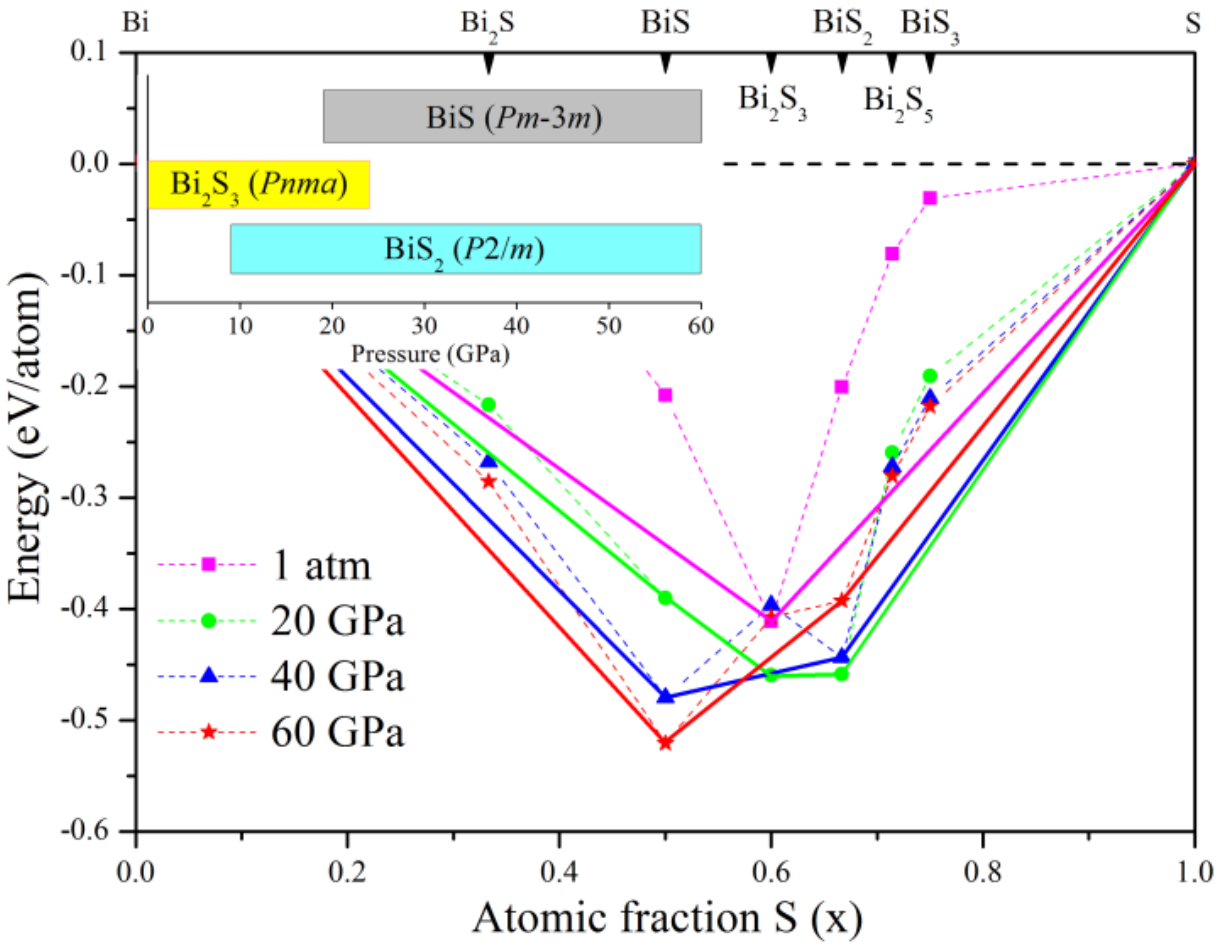

Figure 1: Ground-state and static enthalpy of formation per atom of $Bi_{1-x}S_x$ structures with respect to their end-member compositions; the sulfur molar content (x = 0 corresponds to pure Bi; x = 1 to pure S) for the ground state and P = 1 atm, 20, 40, 60 GPa. The symbols on the solid lines denote that the compounds that we have identified to be stable at the corresponding pressures, while those on the dashed lines represent those that are unstable with respect to decomposition into elements and other stable compounds. The inset shows the stable stoichiometries and their stable range of pressure.

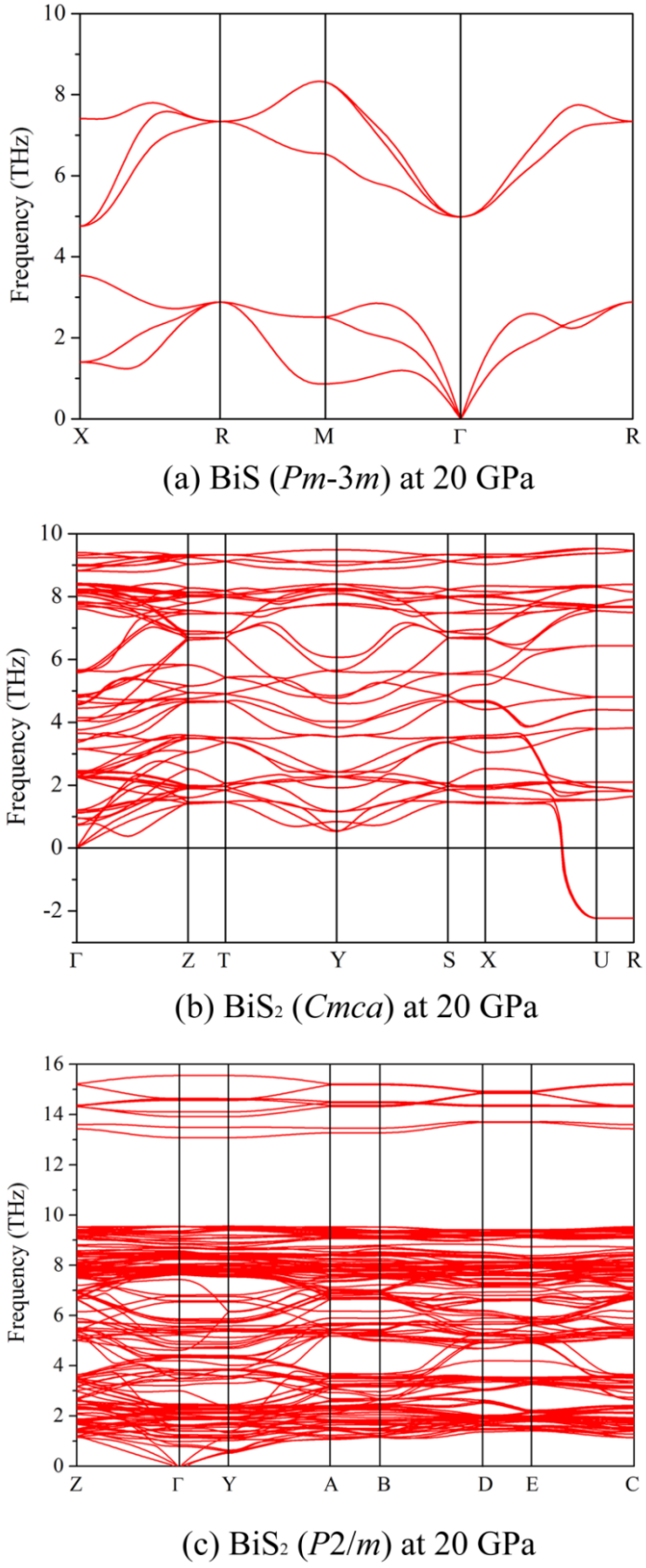

Figure 2: The phonon dispersion curves of (a) BiS (*Pm*-3*m*), (b) BiS_2 (*Cmca*) and (c) BiS_2 (*P*2/*m*) at 20 GPa.

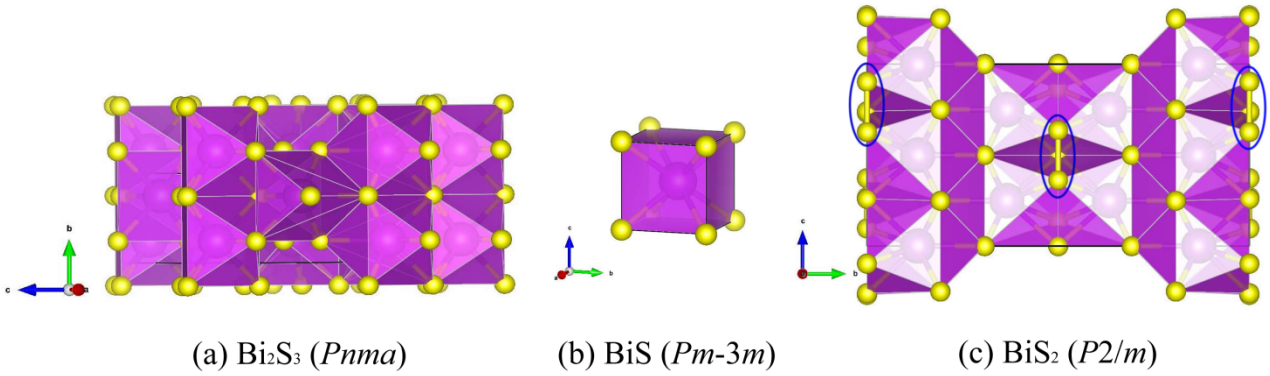

Figure 3: The schematic crystal structures of (a) Bi_2S_3 (*Pnma*), (b) BiS (*Pm*-3*m*) and (c) BiS_2 (*Cmca*) at 20 GPa. Large purple and small yellow spheres represent Bi and S atoms, respectively. The S-S bond is indicated within the blue ellipses.

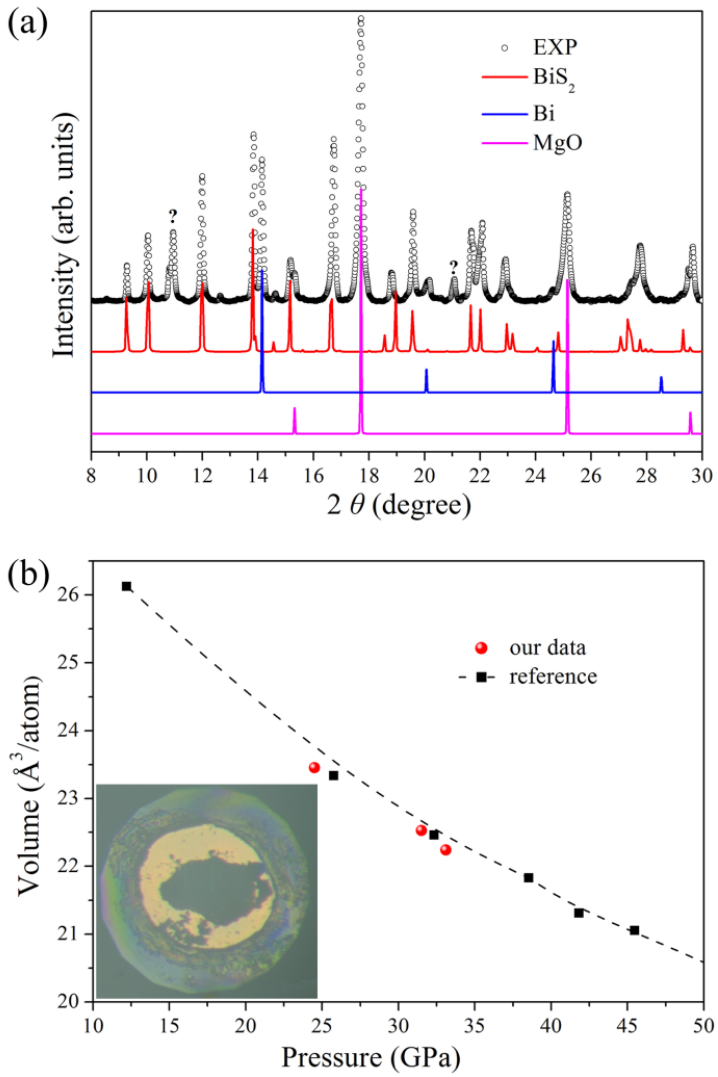

Figure 4: (a) The experimental XRD pattern and the calculated diffraction peaks of BiS_2, Bi and MgO at 31.5 GPa. The unidentified diffraction peaks with question marks are from undefined phases. (b) The red points represent our experimental volume of Bi as a function of pressure compared with the previous equation of state of Bi from the reference [44]. The inset shows the compressed sample in the DAC.

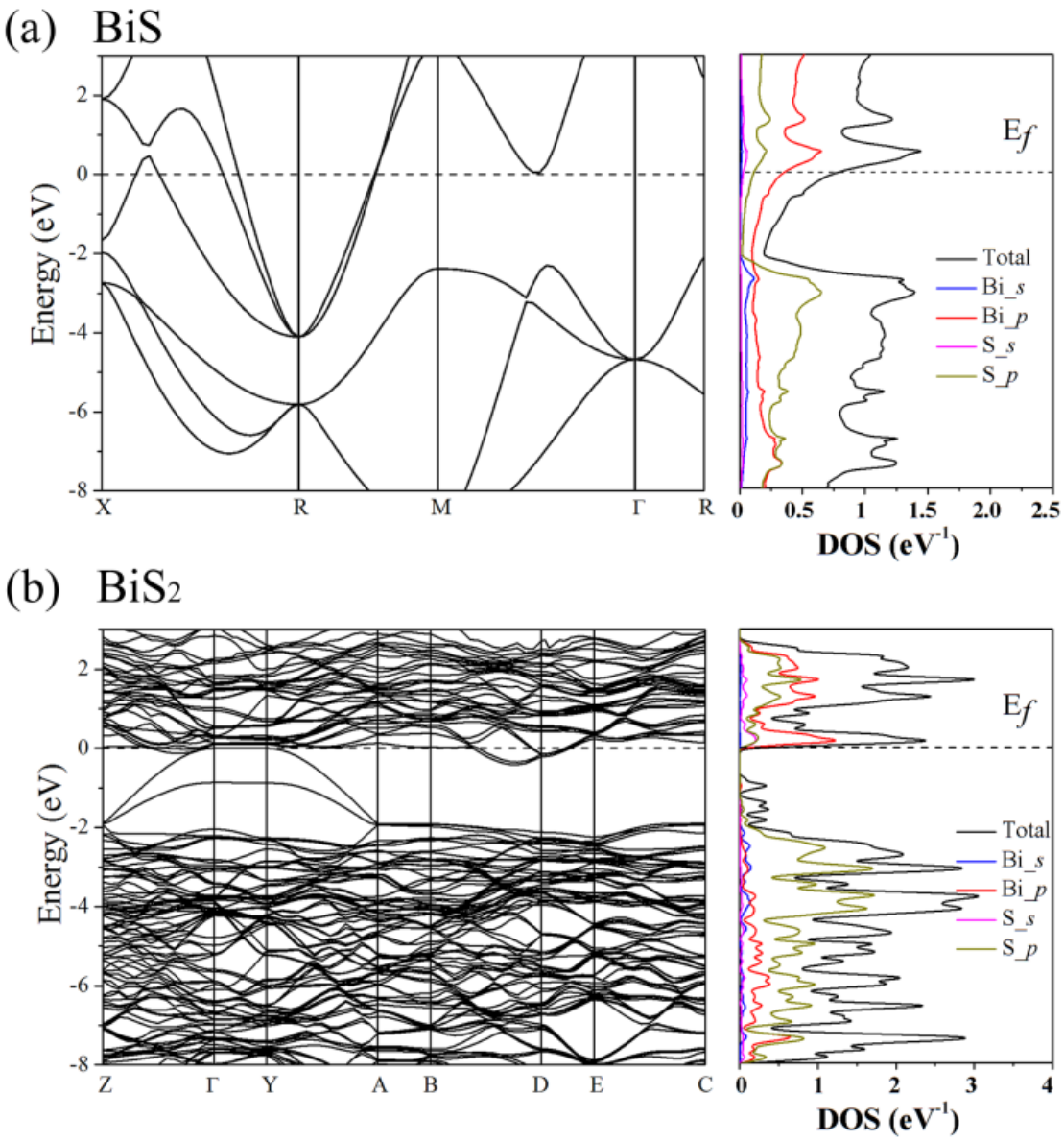

Figure 5: Band structures along high symmetry paths and the projected DOS of (a) BiS and (b) BiS_2 at 20 GPa. The Fermi level has been set to 0 eV.

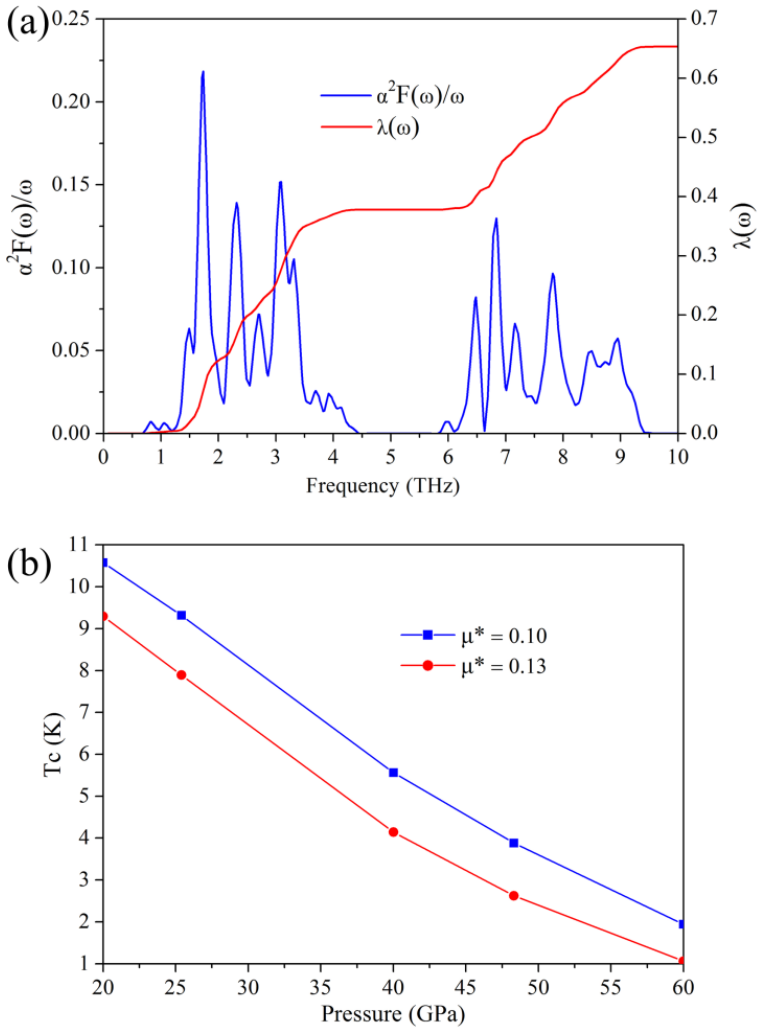

Figure 6: (a) The calculated Eliashberg spectral function $\alpha^2F(\omega)$ and the EPC parameter λ at 20 GPa. (b) The calculated T_c of BiS (*Pm*-3*m*) as a function of pressure.

References

[1] H. Zhang, C.-X. Liu, X.-L. Qi, X. Dai, Z. Fang, and S.-C. Zhang, Nat. Phys. **5**, 438 (2009).

[2] Y. L. Chen, J. G. Analytis, J.-H. Chu, Z. K. Liu, S.-K. Mo, X. L. Qi, H. J. Zhang, D. H. Lu, X. Dai, Z. Fang, S. C. Zhang, I. R. Fisher, Z. Hussain, and Z.-X. Shen, Science (80-.). **325**, 178 (2009).

[3] S. V. Ovsyannikov and V. V. Shchennikov, Chem. Mater. **22**, 635 (2010).

[4] S. V. Ovsyannikov, V. V. Shchennikov, G. V. Vorontsov, A. Y. Manakov, A. Y. Likhacheva, and V. A. Kulbachinskii, J. Appl. Phys. **104**, 53713 (2008).

[5] J. L. Zhang, S. J. Zhang, H. M. Weng, W. Zhang, L. X. Yang, Q. Q. Liu, S. M. Feng, X. C. Wang, R. C. Yu, L. Z. Cao, L. Wang, W. G. Yang, H. Z. Liu, W. Y. Zhao, S. C. Zhang, X. Dai, Z. Fang, and C. Q. Jin, Proc. Natl. Acad. Sci. U. S. A. **108**, 24 (2011).

[6] C. Zhang, L. Sun, Z. Chen, X. Zhou, Q. Wu, W. Yi, J. Guo, X. Dong, and Z. Zhao, Phys. Rev. B **83**, 140504 (2011).

[7] L. Zhu, H. Wang, Y. Wang, J. Lv, Y. Ma, Q. Cui, Y. Ma, and G. Zou, Phys. Rev. Lett. **106**, (2011).

[8] M. Einaga, A. Ohmura, A. Nakayama, F. Ishikawa, Y. Yamada, and S. Nakano, Phys. Rev. B - Condens. Matter Mater. Phys. **83**, (2011).

[9] J. Zhao, H. Liu, L. Ehm, Z. Chen, S. Sinogeikin, Y. Zhao, and G. Gu, Inorg. Chem. **50**, 11291 (2011).

[10] Y. Ma, G. Liu, P. Zhu, H. Wang, X. Wang, Q. Cui, J. Liu, and Y. Ma, J. Phys. Condens. Matter **24**, 475403 (2012).

[11] R. Vilaplana, D. Santamaria-Perez, O. Gomis, F. J. Manjon, J. Gonzalez, a Segura, a Munoz, P. Rodriguez-Hernandez, E. Perez-Gonzalez, V. Marin-Borras, V. Munoz-Sanjose, C. Drasar, and V. Kucek, Phys. Rev. B **84**, 184110 (2011).

[12] G. Liu, L. Zhu, Y. Ma, C. Lin, J. Liu, and Y. Ma, J. Phys. Chem. C **117**, 10045 (2013).

[13] Z. Yu, L. Wang, Q. Hu, J. Zhao, S. Yan, K. Yang, S. Sinogeikin, G. Gu, and H. Mao, Sci. Rep. **5**, 15939 (2015).

[14] M. Miao, Nat. Chem. **5**, 846 (2013).

[15] J. Botana, X. Wang, C. Hou, D. Yan, H. Lin, Y. Ma, and M. Miao, Angew. Chemie **91330**, n/a (2015).

[16] A. Hermann and P. Schwerdtfeger, J. Phys. Chem. Lett. **5**, 4336 (2014).

[17] A. Dewaele, N. Worth, C. J. Pickard, R. J. Needs, S. Pascarelli, O. Mathon, M. Mezouar, and T. Irifune, Nat. Chem. **8**, 2 (2016).

[18] L. Zhu, H. Liu, C. J. Pickard, G. Zou, and Y. Ma, Nat. Chem. **6**, 644 (2014).

[19] A. Dewaele, C. M. Pépin, G. Geneste, and G. Garbarino, High Press. Res. **0**, 1 (2017).

[20] G. Gao, R. Hoffmann, N. W. Ashcroft, H. Liu, A. Bergara, and Y. Ma, Phys. Rev. B **88**, 184104 (2013).

[21] G. Liu, S. Besedin, A. Irodova, H. Liu, G. Gao, M. Eremets, X. Wang, and Y. Ma, Phys. Rev. B **95**, 104110 (2017).

[22] W. Zhang, A. R. Oganov, A. F. Goncharov, Q. Zhu, S. E. Boulfelfel, A. O. Lyakhov, E. Stavrou, M. Somayazulu, V. B. Prakapenka, and Z. Konopkova, Science (80-.). **342**, 1502 (2013).

[23] H. Yu, W. Lao, L. Wang, K. Li, and Y. Chen, Phys. Rev. Lett. **118**, 137002 (2017).

[24] Y. Sharma, P. Srivastava, A. Dashora, L. Vadkhiya, M. K. Bhayani, R. Jain, A. R. Jani, and B. L. Ahuja, Solid State Sci. **14**, 241 (2012).

[25] M. R. Filip, C. E. Patrick, and F. Giustino, Phys. Rev. B **87**, 205125 (2013).

[26] X. Du, F. Cai, and X. Wang, J. Alloys Compd. **587**, 6 (2014).

[27] X. Huang, Y. Yang, X. Dou, Y. Zhu, and G. Li, J. Alloys Compd. **461**, 427 (2008).

[28] Y. Wang, J. Chen, L. Jiang, K. Sun, F. Liu, and Y. Lai, J. Alloys Compd. **686**, 684 (2016).

[29] A. Kyono and M. Kimata, Am. Mineral. **89**, 932 (2004).

[30] L. F. Lundegaard, E. Makovicky, T. Boffa-Ballaran, and T. Balic-Zunic, Phys. Chem. Miner. **32**, 578 (2005).
[31] I. Efthimiopoulos, J. Kemichick, X. Zhou, S. V Khare, D. Ikuta, and Y. Wang, J. Phys. Chem. A **118**, 1713 (2014).
[32] C. Li, J. Zhao, Q. Hu, Z. Liu, Z. Yu, and H. Yan, J. Alloys Compd. **688**, 329 (2016).
[33] Y. Wang, J. Lv, L. Zhu, and Y. Ma, Phys. Rev. B **82**, 94116 (2010).
[34] Y. Wang, J. Lv, L. Zhu, and Y. Ma, Comput. Phys. Commun. **183**, 2063 (2012).
[35] G. Kresse and J. Furthmüller, Phys. Rev. B **54**, 11169 (1996).
[36] E. M. PERDEW J, BURKE K, Phys. Rev. Lett. **77**, 3865 (1996).
[37] L. Kleinman and D. M. Bylander, Phys. Rev. Lett. **48**, 1425 (1982).
[38] A. Togo and I. Tanaka, Scr. Mater. **108**, 1 (2015).
[39] P. Giannozzi, S. Baroni, N. Bonini, M. Calandra, R. Car, C. Cavazzoni, D. Ceresoli, G. L. Chiarotti, M. Cococcioni, I. Dabo, A. Dal Corso, S. de Gironcoli, S. Fabris, G. Fratesi, R. Gebauer, U. Gerstmann, C. Gougoussis, A. Kokalj, M. Lazzeri, L. Martin-Samos, N. Marzari, F. Mauri, R. Mazzarello, S. Paolini, A. Pasquarello, L. Paulatto, C. Sbraccia, S. Scandolo, G. Sclauzero, A. P. Seitsonen, A. Smogunov, P. Umari, and R. M. Wentzcovitch, J. Phys. Condens. Matter **21**, 395502 (2009).
[40] H. K. Mao, J. Xu, and P. M. Bell, J. Geophys. Res. **91**, 4673 (1986).
[41] C. Prescher and V. B. Prakapenka, High Press. Res. **35**, 223 (2015).
[42] K. Aoki, S. Fujiwara, and M. Kusakabe, J. Phys. Soc. Japan **51**, 3826 (1982).
[43] O. Degtyareva, E. Gregoryanz, H.-K. Mao, and R. J. Hemley, High Press. Res. **25**, 17 (2005).
[44] *Y. Akahama, M. Kobayashi, and H. Kawamura, Proceeding of 31st High Pressure Conference of Japan, Osaka, Japan, 1990, Pp. 392–393.* (n.d.).
[45] J. Heyd, G. E. Scuseria, and M. Ernzerhof, J. Chem. Phys. **118**, 8207 (2003).
[46] P. B. Allen and R. C. Dynes, Phys. Rev. B **12**, 905 (1975).

Supplementary Material

Stable Unexpected Stoichiometries of Bismuth Sulfide under High Pressure

Guangtao Liu[1, 2, 3], Zhenhai Yu[1], Hanyu Liu[4], Yanmei Ma[3], Hui Wang[3], Xiaolei Feng[3], Yanming Ma[3, *], Xin Li[1], Ye Yuan[1], Lin Wang[1, *], Ke Yang[5] and Xiaodong Li[6]

[1] *Center for High Pressure Science and Technology Advanced Research, Shanghai 201203, China*

[2] *National Key Laboratory of Shock Wave and Detonation Physics, Institute of Fluid Physics, China Academy of Engineering Physics, Mianyang 621900, China*

[3] *State Key Laboratory of Superhard Materials, Jilin University, Changchun 130012, China*

[4] *Geophysical Laboratory, Carnegie Institution of Washington, Washington, DC 20015, USA*

[5] *Shanghai Institute of Applied Physics, Chinese Academy of Sciences, Shanghai 201203, China*

[6] *Institute of High Energy Physics, Chinese Academy of Sciences, Beijing 100049, China*

Contents

1. The result of molecular dynamics simulation of BiS_2

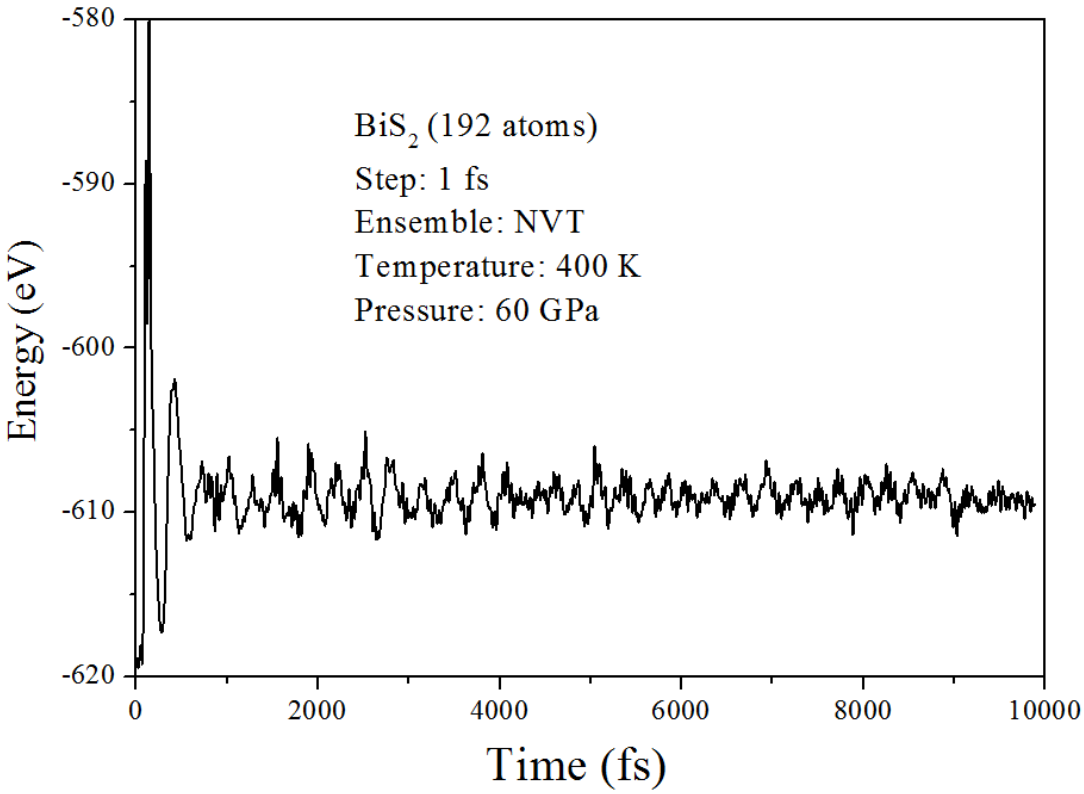

2. The diffraction pattern of Bi_2S_3 with space group of *Pnma* (λ =0.4112 Å).

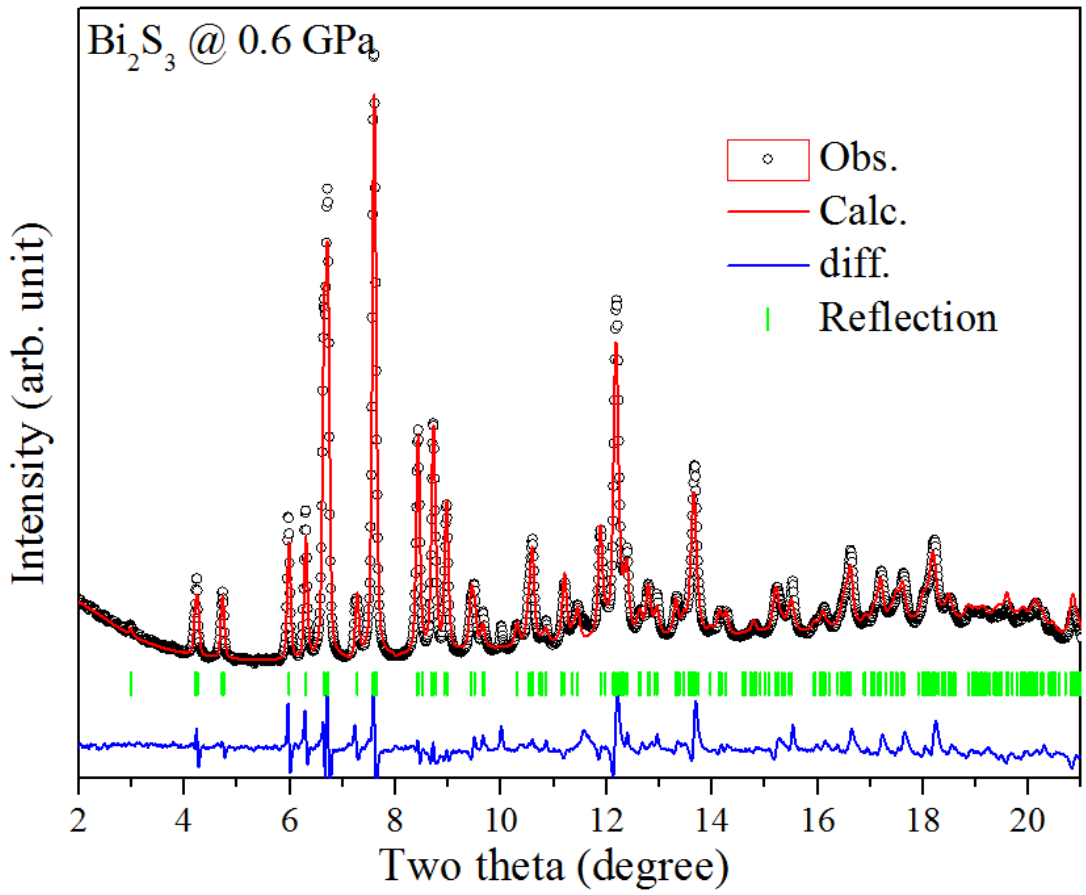

3. The volumes of stoichiometric BiS and BiS_2 as a function of pressure compared with conventional Bi_2S_3.

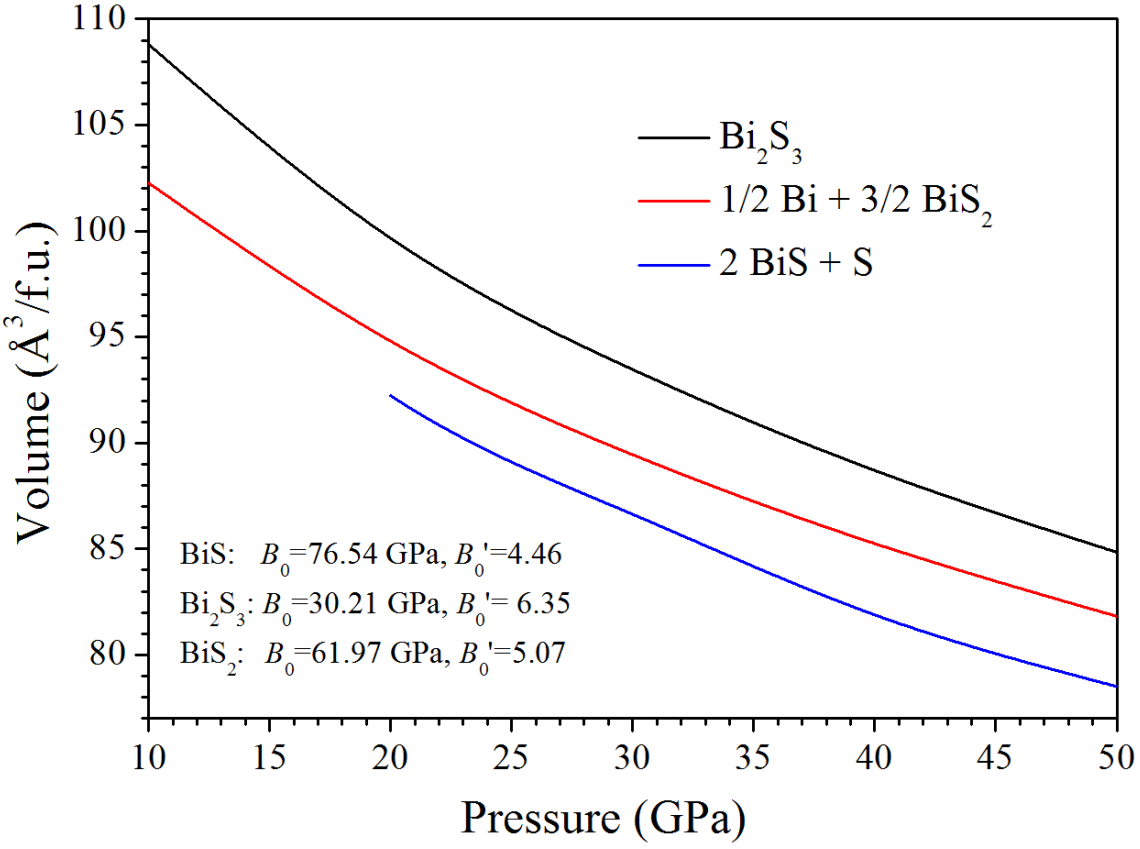

4. The crystal structures of BiS and BiS_2 (VASP file).

(1)
BiS (*Pm*-3*m*) at 20 GPa
1.00000000000000
3.3677745694058010 0.0000000000000000 0.0000000000000000
0.0000000000000000 3.3677745694058010 0.0000000000000000
0.0000000000000000 0.0000000000000000 3.3677745694058014
Bi S
1 1
Direct
0.5000000000000000 0.5000000000000000 0.5000000000000000
0.0000000000000000 0.0000000000000000 0.0000000000000000

(2)
BiS_2 (*Cmca*) at 20 GPa
1.00000000000000
8.2877180174196852 0.0076075151090442 -0.0000000000000000
-6.6092377671773770 5.0004298291723837 0.0000000000000000
0.0000000000000000 0.0000000000000000 5.2828686636001514
Bi S
4 8
Direct
0.1338314231942946 0.8661685768002001 -0.0000000000000000
0.3661685768057053 0.6338314231997999 0.5000000000000000
0.8661685768057052 0.1338314231997999 -0.0000000000000000
0.6338314231942948 0.3661685768002000 0.5000000000000000
0.8637758094917323 0.8637758094929056 0.6366710833080363
0.6362241905082677 0.6362241905070944 0.1366710833080363
0.3637758094917323 0.3637758094929056 0.8633289166919637
0.1362241905082677 0.1362241905070945 0.3633289166919637
0.6920503884911428 0.3079496115094875 -0.0000000000000000
0.8079496115088572 0.1920503884905125 0.5000000000000000
0.3079496115088574 0.6920503884905126 -0.0000000000000000
0.1920503884911426 0.8079496115094874 0.5000000000000000

(3)
BiS_2 (*P*2/*m*) at 20 GPa
1.00000000000000
7.4695029017815759 0.0000000000000000 0.0001721266581011
0.0000000000000000 15.7290289582005816 0.0000000000000000
-0.0031621705658405 0.0000000000000000 7.4629165186663409
Bi S

16 32

Direct

0.2497546534349963 0.6343211826703359 0.2495895637697077
0.7502453315650059 0.3656788173296642 0.7504104512302900
0.7502453315650059 0.6343211826703359 0.7504104512302900
0.2497546534349963 0.3656788173296642 0.2495895637697077
0.7504996609846915 0.3655520564129279 0.2497592695398530
0.2495003390153085 0.6344479435870720 0.7502407004601517
0.2495003390153085 0.3655520564129279 0.7502407004601517
0.7504996609846915 0.6344479435870720 0.2497592695398530
-0.0000000000000000 0.1322200561775630 0.0000000000000000
-0.0000000000000000 0.8677799288224323 0.0000000000000000
0.5000000000000000 0.1352387151868453 0.5000000000000000
0.5000000000000000 0.8647612698131570 0.5000000000000000
-0.0000000000000000 0.8672451460586004 0.5000000000000000
-0.0000000000000000 0.1327548539413925 0.5000000000000000
0.5000000000000000 0.8670127844592701 0.0000000000000000
0.5000000000000000 0.1329872155407299 0.0000000000000000
0.2499631375274615 0.1919305477568808 0.2485205858848810
0.7500368624725384 0.8080694522431192 0.7514793991151212
0.7500368624725384 0.1919305477568808 0.7514793991151212
0.2499631375274615 0.8080694522431192 0.2485205858848810
0.7520912275798993 0.8082014344484304 0.2498925103570578
0.2479087724201006 0.1917985655515696 0.7501075196429446
0.2479087724201006 0.8082014344484304 0.7501075196429446
0.7520912275798993 0.1917985655515696 0.2498925103570578
-0.0000000000000000 0.6927258847259090 0.0000000000000000
-0.0000000000000000 0.3072741152740910 0.0000000000000000
0.5000000000000000 0.6910953283377823 0.5000000000000000
0.5000000000000000 0.3089046716622176 0.5000000000000000
-0.0000000000000000 0.3076083190637379 0.5000000000000000
-0.0000000000000000 0.6923916519362632 0.5000000000000000
0.5000000000000000 0.3078387077379615 0.0000000000000000
0.5000000000000000 0.6921612922620386 0.0000000000000000
0.2741271749991869 0.0000000000000000 0.6273645520905826
0.7258728250008130 0.0000000000000000 0.3726354479094173
0.7349393303990459 0.0000000000000000 0.0967732078860270
0.2650606696009540 0.0000000000000000 0.9032268071139706
0.9093613462173761 0.0000000000000000 0.7404112879729123
0.0906386537826239 0.0000000000000000 0.2595887120270877
0.3647117251838357 0.0000000000000000 0.2683586460731757
0.6352882748161643 0.0000000000000000 0.7316413839268268
0.0000797631866773 0.5000000000000000 0.3635905518888670
0.9999202478133200 0.5000000000000000 0.6364094181111376

0.4998569619383112	0.5000000000000000	0.8635442476155735
0.5001430380616888	0.5000000000000000	0.1364557523844265
0.6363625533069267	0.5000000000000000	0.4996406569713750
0.3636374466930732	0.5000000000000000	0.5003593430286251
0.1363699635099246	0.5000000000000000	0.9996013349378821
0.8636300214900778	0.5000000000000000	0.0003986650621180

5. The convex hull of Bi-Te system at 30 GPa. (Only BiTe and Bi_2Te_3 are considered here.)